Surface Effects on the Physical and Electrochemical Properties of Thin $LiFePO_4$ Particles

K. Zaghib,[†] A. Mauger,*[,‡] F. Gendron,[§] and C. M. Julien[§]

Institut de Recherche d'Hydro-Québec, 1800 Boulevard Lionel Boulet, Varennes, QC, Canada J3X 1S1, Institut de Minéralogie et Physique de la Matière Condensée, UMR 7590, Campus Boucicaut, Université Pierre et Marie Curie, 140 rue de Lourmel, 75015 Paris, France, and Institut des Nano-Sciences de Paris, UMR 7588, Université Pierre et Marie Curie, 140 rue de Lourmel, 75015 Paris, France

Received September 28, 2007. Revised Manuscript Received November 9, 2007

The structure of $LiFePO_4$ particles prepared by a new milling route has been investigated, with emphasis on surface effects found to be important for such small particles, whose sizes were distributed in the range 30–40 nm. The bulk and surface properties of the particles were investigated by a combination of XRD, TEM, FTIR, and magnetic measurements before and after application of a carbon coating intended to optimize the electrochemical performance of the powder used as a cathode element of a new generation of lithium-ion battery. Before the carbon coating was applied, the particles were well-crystallized in the bulk and free from any impurities, but they were surrounded with a disordered, 8 Å thick surface layer in which the iron ions were in the Fe^{3+} low-spin ($S = {}^1/_2$) configuration. Carbon coating at 750 °C reduced the disorder at the surface and switched the Fe^{3+} ions in the surface layer to the high-spin ($S = {}^5/_2$) configuration. These results are discussed with respect to similar effects recently observed for ferrite nanoparticles used in spintronics and biological molecules such as proteins that contain heme Fe.

1. Introduction

$LiFePO_4$ is currently the subject of extensive studies as a positive-electrode material for a new generation of Li-ion batteries. Indeed, it has a low cost, low toxicity, remarkable thermal stability, and a relatively high theoretical specific capacity of 170 mAh/g.[1,2] The early drawback of highly resistive $LiFePO_4$ has been solved by coating the particles with carbon.[3–5] In addition, the material purity is now under control, owing to reduction of iron by hydrogen gas present during the course of the synthesis, either because the samples are prepared by hydrothermal synthesis[6] or because the polymer additive frees hydrogen gas when the samples are prepared by a different chemical route.[7] The current debate in regard to the use of this material in large-size batteries (for hybrid electric vehicles, for instance) is now mainly focused on attempts to increase the rate capability. This goal can be achieved by decreasing the size of the particles as much as possible, in order to increase the effective surface area that is active for electrochemical reactions. Yet attention must be paid to the quality of the surface, especially as the importance of the surface-to-volume ratio increases, in order to prevent the surface from acting as a barrier to transfer of lithium ions and/or electrons during the charging and discharging of lithium batteries. In this context, we report here the characterization of the surface of $LiFePO_4$ particles prepared by solid-state reaction and having diameters (d) of 35 ± 5 nm.

The bulk properties of the particles were characterized by powder X-ray diffraction (XRD) analysis, transmission electron microscopy (TEM), Fourier-transform infrared (FTIR) spectroscopy, and magnetic measurements. The lattice coherence length, deduced from the XRD analysis using the Scherrer equation, was comparable to the size of the particles detected by TEM, showing that the material was well-crystallized. The FTIR spectra and analysis of the magnetization curves showed that no impurity phase poisoned the material.

The surface of the particles was analyzed at two stages of the preparation of the samples: after the solid-state polymeric synthesis but before ball milling and after ball milling followed by application of the final carbon coating. We refer to these particles as uncoated and coated particles, respectively. We have recently argued that magnetic properties are a suitable tool for characterizing the intrinsic bulk properties of $LiFePO_4$ particles.[8] We used the same technique here to characterize the surface of the particles. The magnetic response of the uncoated particles gave evidence of a spin-disordered surface layer in which iron was in the Fe^{3+} low-spin state. The presence of Fe^{3+} at the surface seems to be

* To whom correspondence should be addressed.
[†] Institut de Recherche d'Hydro-Québec.
[‡] Institut de Minéralogie et Physique de la Matière Condensée.
[§] Institut des Nano-Sciences de Paris.

(1) Padhi, A. K.; Nanjundaswamy, K. S.; Goodenough, J. B. *J. Electrochem. Soc.* **1997**, *144*, 1188.
(2) Ravet, N.; Chouinard, Y.; Magnan, J. F.; Besner, S.; Gauthier, M.; Armand, M. *J. Power Sources* **2001**, *144*, 1188.
(3) Ravet, N.; Abouimrane, A.; Armand, M. *J. Power Sources* **2001**, *97–98*, 503.
(4) Ravet, N.; Besner, S.; Simoneau, M.; Vallée, A.; Armand, M.; Magnan, J. F. *U.S. Patent*6,962,666, 2005.
(5) Hu, Y.; Doeff, M. M.; Kostecki, R.; Finones, R. *J. Electrochem. Soc.* **2004**, *151*, A1279.
(6) Chen, J.; Whittingham, M. S. *Electrochem. Commun.* **2006**, *8*, 855.
(7) Ravet, N.; Gauthier, M.; Zaghib, K.; Goodenough, J. B.; Mauger, A.; Gendron, F.; Julien, C. M. *Chem. Mater.* **2007**, *19*, 2595.
(8) Julien, C. M.; Mauger, A.; Ait-Salah, A.; Massot, M.; Gendron, F.; Zaghib, K. *Ionics* **2007**, *13*, 395, and references therein.

10.1021/cm7027993 CCC: $40.75
Published on Web 12/15/2007

an intrinsic property of $LiFePO_4$, and its appearance in this work conciliates the structural, chemical, and physical properties that probe the core region of these particles with Mössbauer spectroscopy measurements reported in the literature that systematically detected an unexpected small percentage of Fe^{3+} ions. The results can be compared with those for ferrite nanoparticles, which are also iron−oxygen-based compounds that show a core region formed by spins with antiferromagnetic interactions surrounded by a magnetically disordered shell. The similitude between $LiFePO_4$ and the ferrite nanoparticles suggests that the surface should be very sensitive to both the mode of preparation and the carbon coating. The study of biological molecules in which Fe^{3+} plays an important catalytic role at the surface also suggests that the state (either low- or high-spin Fe^{3+}) should very much depend on the carbon deposit. This was corroborated by the magnetic study of the surface of the same particles after they were carbon-coated using lactose as the carbon additive. No evidence of low-spin Fe^{3+} at the surface was detected in this latter case, suggesting that the trivalent iron ions in the surface layer of the coated particles were in the high-spin state after carbon coating.

Electrochemical properties were also investigated before and after carbon coating. After the particles were carbon-coated, their coulomb efficiency was close to 100%, and their properties were in agreement with those we previously published for our samples now used for commercial purposes. On the other hand, before the carbon coating was applied, the electronic performance was degraded even at the very slow charge/discharge rate (C/24) that we chose in order to be as close to thermodynamic equilibrium as possible. In particular, the charge/discharge curves of $LiFePO_4$/$LiPF_6$−EC−DEC/Li cells (EC = ethylene carbonate, DEC = diethylene carbonate) showed finite slopes over a broad region, in contrast to the plateau at 3.5 V characteristic of this kind of cell after carbon coating of the particles (replacing $LiFePO_4$ by C-$LiFePO_4$). This result showed that the carbon coating not only improved the performance of the cell by improving the electronic conductivity but also reduced the surface disorder, thus favoring the two-phase system $xLiFePO_4 + (1 - x)FePO_4$ with respect to the homogeneous phase.

In addition, we found that the magnetic properties can be used as a means of characterizing the surface, opening a new field of investigation that involves relating the surface effects to the mode of preparation in order to optimize electron and ion transport through the surface, thereby improving the electrochemical properties of this most promising material in the near future.

2. Experimental Procedures

Synthesis. The $LiFePO_4$ particles were prepared by a solid-state reaction at 700 °C under an inert (nitrogen) atmosphere using the polymeric synthetic route described elsewhere.[10] The starting materials were iron(III) phosphate ($FePO_4 \cdot 2H_2O$) and lithium carbonate (Li_2CO_3) as precursors. To obtain nanosized particles, the $LiFePO_4$ powders were ball-milled in a liquid solution containing isopropyl alcohol under an inert atmosphere. The particles obtained after drying could be considered as uncoated particles because of the great damage caused by the ball-milling process. Carbon-coated particles were obtained using lactose as the carbon precursor in acetone solution, according to the following procedure. The uncoated particles were mixed with the carbon precursor. The dry additive corresponded to 5 wt % carbon in $LiFePO_4$. After it was dried, the blend was heated at 750 °C for 4 h under an argon atmosphere. The quantity of carbon represented about 1 wt % of the material (C-detector, LECO Co., CS 444).

Structural Characterization. The crystal structure of the particles was analyzed by XRD with a Philips X'Pert apparatus equipped with a Cu Kα X-ray source (λ = 1.5406 Å). XRD measurements were collected in a 2θ range of 10–80° in step-scanning mode [$\Delta(2\theta) = 0.05°$]. The structural parameters were determined by Rietveld refinement of the diffraction profiles. High-resolution transmission electron microscopy (HRTEM) images were obtained using an electronic microscope (Hitachi model H-9000) working at a potential of 300 kV. The TEM samples were ultrasonically treated in a solution of isopropyl alcohol and then deposited on a silica substrate.

Physical Characterization. FTIR absorption spectra were recorded with a Fourier-transform interferometer (Bruker model IFS113v) over a wavenumber range of 150–1400 cm^{-1} at a spectral resolution of 1 cm^{-1}. Magnetic measurements (susceptibility and magnetization) were carried out using a fully automated magnetometer (Quantum Design MPMS-5S) with a superconducting quantum interference device (SQUID) over a temperature range of 4–300 K.

Electrochemistry. The electrochemical experiments were carried out in cells in which metallic lithium served as the negative electrode using the coffee-bag technology developed at Hydro-Quebec and described elsewhere.[9] The electrolyte was 1 M $LiPF_6$ in 1/1 EC/DEC solvent (Merck LP40). The cell was charged and discharged at a rate of C/24 before and after carbon coating. All of the electrochemical properties reported here were measured at room temperature.

3. Structure and Morphology

The XRD pattern (not shown here) was in agreement with the results we reported in previous work on $LiFePO_4$. All of the diffraction lines could be indexed in the orthorhombic system with the *Pmma* space group. The refined lattice parameters were a = 10.3298(2) Å, b = 6.0097(8) Å, c = 4.693(1) Å, and V = 291.3(3) $Å^3$, all of which were in good agreement with the literature values.[11,12] The average monocrystallite diameter (d) was calculated from the XRD line width using the Scherrer equation, $d = 0.9\lambda/(\beta_{1/2} \cos \theta)$, where λ is the X-ray wavelength, $\beta_{1/2}$ is the corrected width at half-maximum of the diffraction peak, and θ is the diffraction angle. Values of d were measured for different angles corresponding to the (200), (101), (111), (211), and (311) lines. No significant dependence on θ was observed, and the overall result was $d = 35 \pm 5$ nm.

The typical TEM image displayed in Figure 1 shows that the powders were composed of well-dispersed secondary particles that were slightly agglomerated and a small quantity

(9) Zaghib, K.; Shim, J.; Guerfi, A.; Charest, P.; Striebel, K. A. *Electrochem. Solid-State Lett.* **2005**, *8*, A207.
(10) Zaghib, K.; Mauger, A.; Goodenough, J. B.; Gendron, F.; Julien, C. M. *Chem. Mater.* **2007**, *19*, 3740.
(11) Streltsov, V. A.; Belokoneva, E. L.; Tsirelson, V. G.; Hansen, N. K. *Acta Crystallogr.* **1993**, *B49*, 147.
(12) Andersson, A. S.; Thomas, J. O. *J. Power Sources* **2001**, *97–98*, 498.

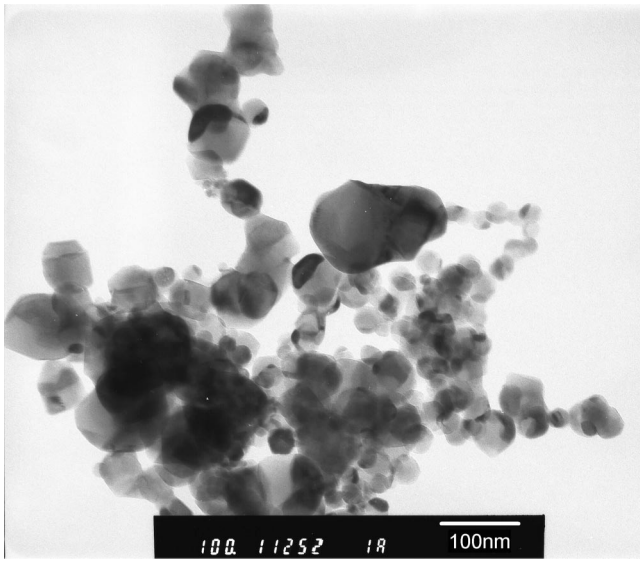

Figure 1. TEM image of $LiFePO_4$ particles before carbon coating.

of isolated primary particles. The average size of the primary particles was found to be 45 nm, only slightly larger than the value of the coherence length deduced from the Scherrer equation, which gives evidence that the primary particles are very well crystallized. HRTEM images in Figure 2 show that the particles had lost their carbon coat after ball-milling and possessed a surface roughness that was cured after the particles were coated again.

FTIR spectroscopy is a probe of vibrations of molecular edifices and is thus a good means of investigating the structure on a local scale. The FTIR spectrum of our sample is shown in Figure 3. The spectrum of $LiFePO_4$ has already been reported and analyzed elsewhere[13,14] and consists of many bands whose positions have been labeled in Figure 3. This labeling shows that only bands intrinsic to $LiFePO_4$ were observed, giving evidence that no impurity phase poisoned the material.[7] The modes ranging from 372 to 1139 cm^{-1} are internal modes that originate from the intramolecular vibrations of the PO_4^{3-} oxyanion. They involve the displacement of oxygen atoms at frequencies closely related to those of the free molecule, which explains why this part of the spectrum was not sensitive to any surface effects and was found to be the same as that of bulk $LiFePO_4$. The gap between 700 and 900 cm^{-1} separates the P−O stretching modes in the range 945–1139 cm^{-1} from the O−P−O bending modes in the range 372–647 cm^{-1}. In well-crystallized samples without impurities, this gap is a flat region of the spectrum having a very small absorbance, which means that this region is a probe for impurities and defects in the crystal structure. In the present case, no band characteristic of P_2O_7 units was observed in this region. However, this part of the spectrum was not flat but rather showed a continuous nonvanishing background that increased smoothly in the direction of decreasing wavenumber. Such a feature has also been observed in the FTIR spectrum of $LiFePO_4$ particles in an early stage of the synthesis of the material (i.e., at a stage where the $LiFePO_4$ was not yet entirely crystallized)[7] as well as in amorphous $LiFePO_4$.[15] This feature thus suggests the existence of a poorly crystallized region. Since, however, the coherence length of the lattice was comparable to the particle size, the disorder was not distributed inside the particles and should thus have been a surface effect. This was confirmed by magnetization measurements, as discussed in the next section.

The external vibrational modes or lattice modes are located at wavenumbers smaller than 400 cm^{-1}. This part of the spectrum was unchanged with respect to that of bulk $LiFePO_4$. This is additional evidence that the core region of the particles was well-crystallized and not affected by size or surface effects.

4. Magnetic Properties

Magnetization curves $M(H)$ of the uncoated particles at different temperatures are shown in Figure 4. M is linear in H over the whole range of magnetic fields investigated ($H \leq 30$ kOe) in the paramagnetic regime ($T > 52$ K). Only at the lowest temperature investigated, $T = 4$ K, was a negative curvature of the magnetization curve detected. This is direct evidence that neither Fe_2O_3 nor Fe_2P impurity phases existed in this sample.[17,18] In addition, this linear behavior justifies the definition of the magnetic susceptibility, $\chi = M/H$, measured at $H = 10$ kOe. The results of the χ measurements are reported in Figure 5 as $\chi^{-1}(T)$ in order to analyze the Curie–Weiss behavior. The relative minimum in $\chi^{-1}(T)$ corresponds to the Néel temperature (T_N) of 52 K characteristic of $LiFePO_4$.[18] For $T > T_N$, the quasi-linear variation of $\chi^{-1}(T)$ shows that the Curie–Weiss law was satisfied:

$$\chi(T) = \frac{C}{T + \theta_p}, \quad C = \frac{4S(S+1)\mu_B}{3k_B} \qquad (1)$$

with conventional notations. Here we have taken into account the fact that the crystal field quenches the orbital momentum of the iron. In pure bulk $LiFePO_4$, the iron is in the high-spin state of the Fe^{2+} configuration ($S = 2$), so that the Curie constant is $C = 3.00$ emu K/mol, which corresponds to an effective magnetic moment $\mu_{eff} = 2[S(S+1)]^{1/2}\mu_B = 4.90\mu_B$. This value of μ_{eff} in eq 1 quantitatively fits the experimental results for $LiFePO_4$ samples that satisfy the purity and stoichiometry requirements. The value of 2.72 emu K/mol for the Curie constant deduced from the slope of the experimental $\chi^{-1}(T)$ curve in Figure 5, however, was quite small and corresponded to an unphysical magnetic moment of $4.66\mu_B$.

Impurity phases in bulk $LiFePO_4$, when they exist, always lead to an effective Curie constant greater than 3.00 emu K/mol.[15,16,19] Stoichiometric deviations have the same effect.[10] The smaller value of C or μ_{eff} in the present sample must have had another origin, namely, a dramatic decrease

(13) Paques-Ledent, M. T.; Tarte, P. *Spectrochim. Acta* **1974**, *A30*, 673.
(14) Burma, C. M.; Frech, R. *J. Electrochem. Soc.* **2004**, *151*, 1032.
(15) Ait-Salah, A.; Jozwiak, P.; Zaghib, K.; Garbarczyk, J.; Gendron, F.; Mauger, A.; Julien, C. M. *Spectrochim. Acta* **2006**, *A65*, 1007.
(16) Ait-Salah, A.; Mauger, A.; Julien, C. M.; Gendron, F. *Mater. Sci. Eng., B* **2006**, *129*, 232.
(17) Ait-Salah, A.; Mauger, A.; Zaghib, K.; Goodenough, J. B.; Ravet, N.; Gauthier, M.; Gendron, F.; Julien, C. M. *J. Electrochem. Soc.* **2006**, *153*, A1692.
(18) Santoro, R. P.; Newnham, R. E. *Acta Crystallogr.* **1967**, *22*, 344.
(19) Mauger, A.; Ait-Salah, A.; Gendron, F.; Massot, M.; Zaghib, K.; Julien, C. M. *ECS Trans.* **2007**, *3*, 115.

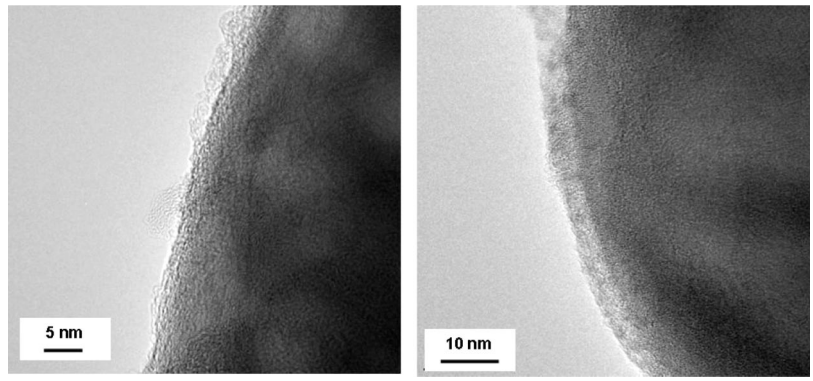

Figure 2. HRTEM images of the surface of a $LiFePO_4$ particle before carbon coating (left) and after carbon coating (right). The lighter region surrounding the particle (darker region) is the carbon layer, which is a few nanometers thick in the right picture. This lighter region in the image to the left is residual carbon remaining only at several spots on the surface, most of the carbon having been removed by the ball-milling process.

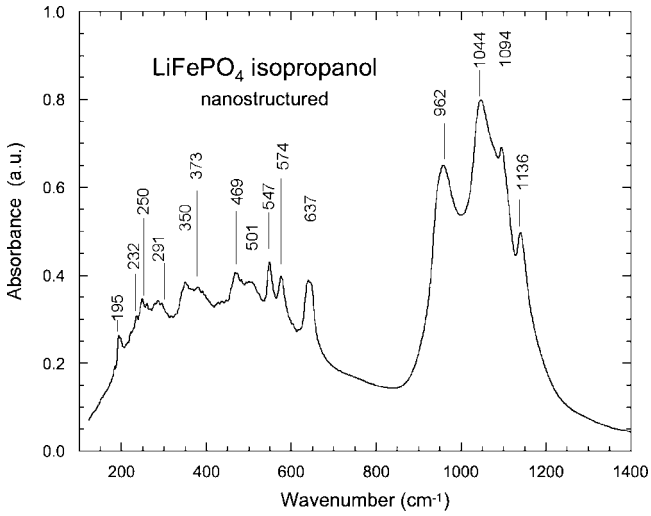

Figure 3. FTIR spectrum of the $LiFePO_4$ sample before carbon coating. Vertical lines indicate the positions (in cm^{-1}) of the intrinsic modes of bulk $LiFePO_4$.

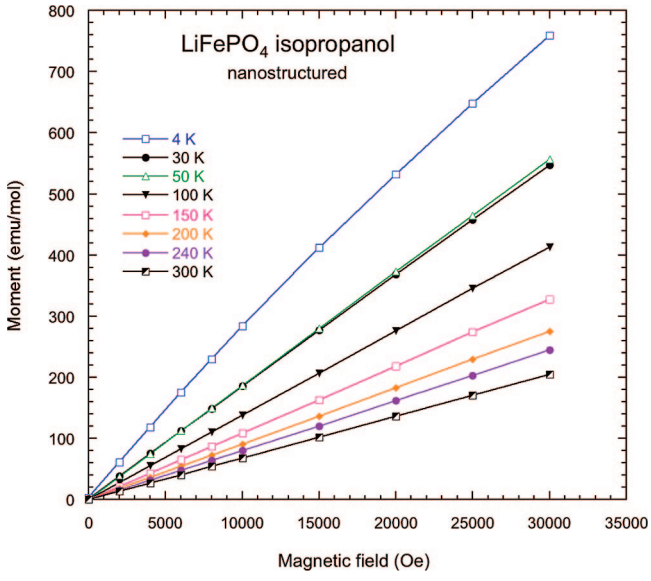

Figure 4. Magnetization curves of the $LiFePO_4$ sample at different temperatures before carbon coating.

in the contribution to χ of the iron atoms at the surface of the $LiFePO_4$ particles. This effect could be modeled by a

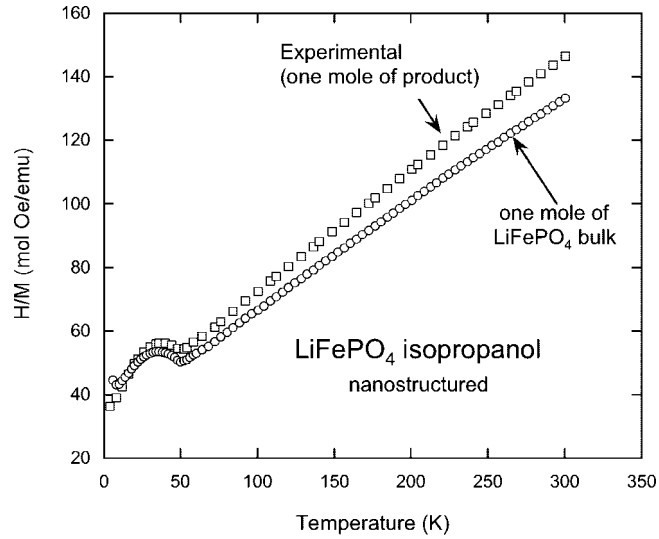

Figure 5. Plots of the inverse of the magnetic susceptibility as a function of temperature for the $LiFePO_4$ sample (open squares) and the $LiFePO_4$ core region of the particles (open circles) before carbon coating. The symbols are experimental data. Only half of the sample data have been included, in order to improve the clarity of the figure. The open circles were obtained from the rough data by subtracting the contribution of the surface layer of the particles as explained in the text. The contribution of the core was normalized to 1 mol of the core region rather than to 1 mol of the sample (core plus surface layer) in order to emphasize the distortion of the magnetic response resulting from the existence of the surface layer (in particular, the change of the slope in the paramagnetic regime).

decomposition of the experimental value of $\chi(T)$ into two components:

$$\chi(T) = y\frac{C_0}{T + \theta_0} + (1 - y)\frac{C'}{T} \qquad (2)$$

The first component gives the contribution of the core region of the $LiFePO_4$ particles, and the second term describes the contribution of the Fe atoms in the surface layer of the particles. The symbol y denotes the fraction of iron ions in the bulk. We knew from the XRD and FTIR experiments reported in the previous section that the core region was not affected by any size effect of the particle, so the respective values of the parameters C_0 and θ_0 that were relevant for this material were 3.00 emu K/mol and 101 ± 6 K, depending on the authors. The second component is the contribution of Fe spins in the surface layer. Because of the increased frustration of these spins near the surface, they

were assumed to be uncorrelated, so that their contribution to the magnetic susceptibility satisfied the Curie law. We were then left with two fitting parameters, namely, C', which depends on the spin carried by the Fe atoms in the surface layer, and y, the fraction of Fe atoms in the bulk. A nonunique but convenient way to analyze eq 2 consisted of choosing sets of two temperatures indexed by the subscript i, say $(T_i, 2T_i)$, satisfying the conditions 100 K $< T_i$ and $2T_i <$ 300 K. Then, from eq 2,

$$2\chi(2T_i) - \chi(T_i) = y\left(\frac{2C_0}{2T_i + \theta_0} - \frac{C_0}{T_i + \theta_0}\right) \qquad (3)$$

Substituting the values $C_0 = 3.00$ emu K/mol and $\theta_0 = 101$ K into eq 3 provided us with the value y_i of y. Then y was the average of the set $\{y_i\}$. This procedure had an advantage: it yielded the value of y without the need for a hypothesis on C' and thus on the configuration of Fe in the surface layer. The result was $y = 0.89$. Given this value, it was straightforward to determine C' from the fit of the experimental $\chi(T)$ curve to eq 2. The result was $C' = 0.37$ emu K/mol, which corresponds to a spin of $S = {}^1/_2$, implying that the iron ions in the surface layer were Fe^{3+} ions in the low-spin state.

It should be noted that this analysis, which allowed us to demonstrate the presence of Fe^{3+} ions and determine their concentration, was performed in the paramagnetic regime, where the Curie–Weiss law applies. However, the contribution of $Fe^{3+}(S = {}^1/_2)$ also affected the magnetic properties at temperatures below T_N. Actually, this contribution became much more important at low temperatures because of the T^{-1} divergence of the Curie law at $T = 0$, as evidenced in Figure 5 by the quasi-linear decrease of the experimental $\chi^{-1}(T)$ curve upon cooling from 50 to 4 K. This was pathologic behavior that was not observed in $LiFePO_4$ powders prepared with particles of larger size and a different surface treatment that prevented such surface effects.[16,17,19] In those cases we had investigated in the past, the minimum in $\chi^{-1}(T)$ at T_N was more pronounced, and a small decrease of $\chi^{-1}(T)$ upon cooling, if any, was observed only at low temperature. We have found in the present case that the $Fe^{3+}(S = {}^1/_2)$ ions are entirely responsible for the dramatic increase of the magnetic susceptibility below T_N. This is evidenced in Figure 6, which shows the experimental susceptibility curve along with the bulk contribution deduced by subtracting from the experimental signal the second term of eq 2 using the values $C' = 0.37$ emu K/mol and $y = 0.89$ determined from the high-temperature analysis. We found that this bulk contribution demonstrated the standard behavior of antiferromagnetic $LiFePO_4$ and saturated to a value of 2×10^{-2} emu/mol of product at low temperature.

The value of y that accounts for the deviation of the experimental magnetic susceptibility from that of bulk $LiFePO_4$ in the paramagnetic regime is thus also the value that cancels the T^{-1} divergence of $\chi(T)$ in the antiferromagnetic phase of the core upon cooling to 4 K. This self-consistence in the description of the magnetic properties on both sides of T_N is a test of the validity of the model, just as in the case of the detection of impurity phases.[19]

The inverse of the magnetic susceptibility of the coated particles as a function of temperature is displayed in Figure 7, together with that of the particles before carbon coating. The magnetic response of the coated particles was closer to the result predicted for intrinsic $LiFePO_4$ [given by the $\chi(T)$ curve after deduction of the surface contribution, shown in Figure 6]; however, the effective moment of $5.02\mu_B$ was still slightly larger than the theoretical value of $4.90\mu_B$. Since Fe^{3+} in the high-spin state has $S = {}^5/_2$, its effective moment would be $5.92\mu_B$, and we note that

$$y(4.9)^2 + (1 - y)(5.92)^2 = (5.02)^2 \qquad (4)$$

which means that the excess in magnetic moment with respect to the theoretical value was entirely attributable to the conversion of $Fe^{3+}(S = {}^1/_2)$ to $Fe^{3+}(S = {}^5/_2)$ in the surface layer.

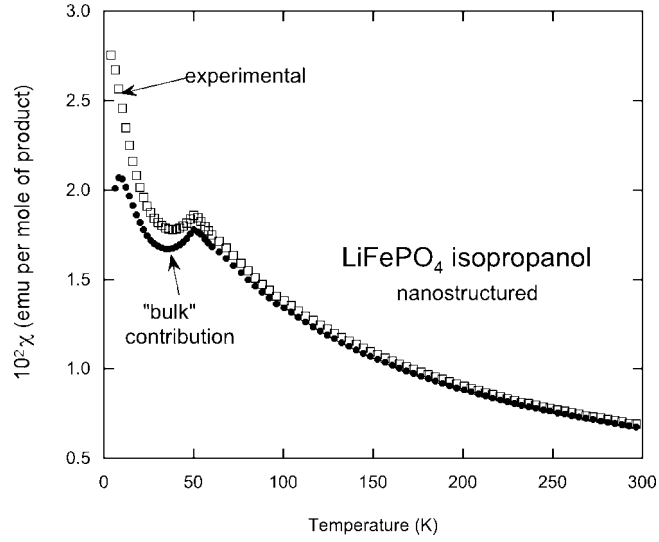

Figure 6. Magnetic susceptibility curve of the $LiFePO_4$ particles before carbon coating. Open squares represent rough data, only half of which have been reported in order to improve clarity. Solid circles represent the contribution from the core region of the particles. The difference is the contribution of the surface layer of the particles.

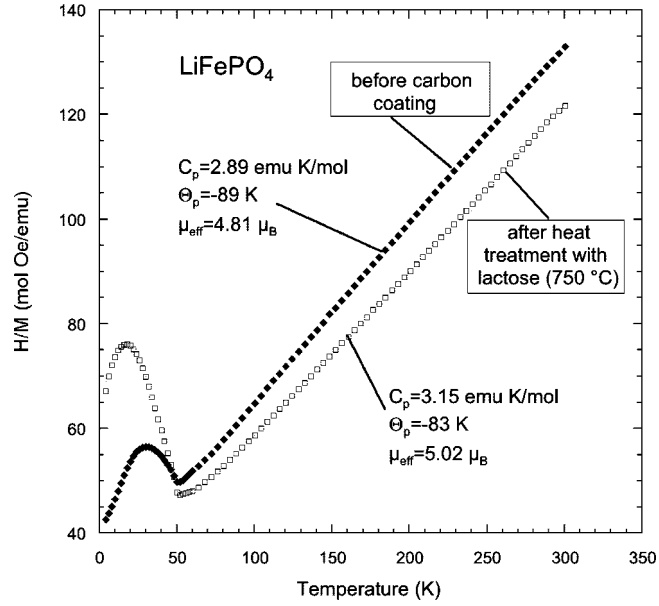

Figure 7. Plots of the inverse of the magnetic susceptibility before and after carbon coating as a function of temperature.

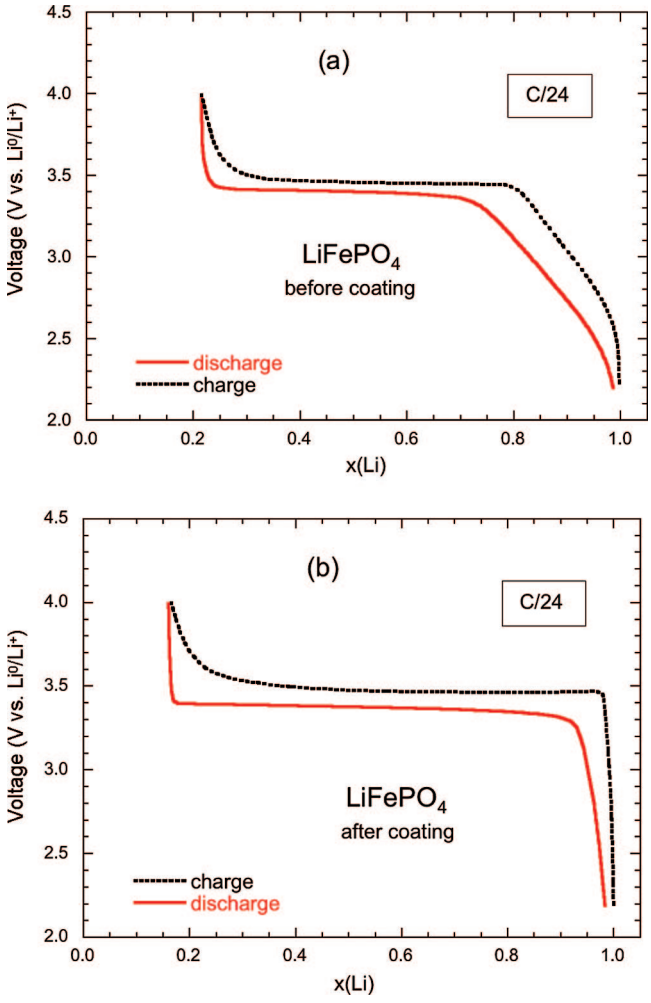

Figure 8. Charge–discharge voltage profiles of $LiFePO_4$ obtained using an $LiFePO_4/LiPF_6$−EC−DEC/Li cell at room temperature (a) before and (b) after carbon coating of the cathode material. The test was performed galvanostatically at a charge–discharge rate of C/24.

5. Electrochemical Properties

Figure 8 shows typical charge–discharge voltage profiles of the $LiFePO_4$ cathode material investigated here, obtained (a) before and (b) after carbon coating using an $LiFePO_4/LiPF_6$−EC−DEC/Li cell. The tests were performed galvanostatically at a charge–discharge rate of C/24 in the voltage range 2.2–4.0 V versus Li^0/Li^+. The charge–discharge profile appears with the typical voltage plateau (at 3.45 V vs Li^0/Li^+) attributed to the two-phase reaction of the $(1 - x)FePO_4 + xLiFePO_4$ system. The carbon-coated material exhibited a reversible capacity of 160 mAh/g, corresponding to a utilization efficiency of 94%. Before the carbon coating was applied, however, the width of the plateau was smaller. In Figure 8b, there is a significant slope in the voltage−capacity curve (with capacity expressed in terms of the Li concentration x) over the range $0.8 < x < 1$ during the charge step and over the extended range $0.7 < x < 1$ during the discharge step. It is commonly believed that reducing the size of the $LiFePO_4$ particles may affect the phase diagram of the $FePO_4/LiFePO_4$ system and favors the existence of the solid solution Li_xFePO_4. However, we can see from the present study and Figure 8b that decreasing the particle size even to values as small as 30–40 nm did not reduce the extension of the plateau and thus did not affect the phase diagram of $FePO_4/LiFePO_4$, which remained a two-phase system. The slope in Figure 8a was observed on the same particles before carbon coating, even though the cycles were purposely done very slowly, at a rate of C/24, in order to remain as close as possible to thermodynamic equilibrium. This was thus a surface effect, which suggests that the amorphous surface layer containing $Fe^{3+}(S = {}^1/_2)$ allows a more homogeneous distribution of Li and Li vacancies upon delithiation than the crystal, where iron is in the $Fe^{2+}(S = 2)$ state. The carbon coating used to increase the electronic conductivity thus also has the major advantage of curing the surface disorder.

6. Discussion

Our experimental setup did not allow us to cool the sample below 4 K. According to eq 2, the T^{-1} divergence of the magnetic susceptibility upon cooling below 4 K should prevail at very low temperatures because it could be removed only by a determination of C' to an infinite number of decimal places in the limit $T \rightarrow 0$. The model, however, should no longer be valid as $T \rightarrow 0$, because the $Fe^{3+}(S = {}^1/_2)$ spins would most likely undergo a transition to a spin-glass phase so that the magnetic susceptibility could remain finite. Such a spin-glass ordering near the surface of antiferromagnetic small particles has been investigated both experimentally and theoretically. From an experimental point of view, surface spin disorder has been observed and investigated mostly on nanosized ferrite particles because they are of particular interest for the development of high-density magnetic storage. Such particles are ferrimagnetic, but the spin topologies of ferri- and antiferromagnetic particles are the same, since in both cases the magnetic order in the bulk involves negative exchange couplings and can be described by two or more sublattices with moments in different directions. For such a topology, the lower coordination of the spins at the surface and/or the reduced mean field is sufficient to induce surface spin disorder,[20] so that no distinction need be made between ferri- and antiferromagnetic particles regarding spin-disorder effects. Spin-glass surface disorder of antiferromagnetic particles has been modeled, for instance, in ref 20. Since the second term in eq 2 has been found to be valid down to 4 K, the spin-glass transition of the surface layer must occur at a temperature $T_g \leq 4$ K. This small value of T_g shows that the magnetic coupling energy per spin (E_m) between spins at the surface is small, since magnetic freezing typically occurs when this magnetic energy overcomes the thermal fluctuations: $k_B T_g \approx E_m$. This is actually expected because the spin carried by the iron ions in the surface layer is $S = {}^1/_2$, instead of $S = 2$ as in the core. Since the magnetic energy is proportional to S^2 and the spin freezing takes place when the magnetic energy overcomes the thermal energy $k_B T$, this simple change in the spin magnitude implies a reduction of T_g by a factor of 16 with respect to T_N, so that we would expect $T_g \approx 3$ K for a thick spin-disordered layer. In the case of a single

(20) Souza Leite, V.; Figueredo, W. *Phys. A* **2005**, *350*, 379.

atomic layer, the $S = {}^1/_2$ spins on the surface would be coupled with the $S = {}^5/_2$ spins of the inner atomic shells, so that the reduction factor of T_g with respect to T_N would be only 4 instead. However, in that case, an additional factor of 2 would come from the change in the coordination number, so that T_g would be on the order of 6 K, although this is an overestimation because this very crude estimate neglects surface magnetic anisotropy effects as well as the effects of geometric disorder due to amorphization of the surface layer suggested by the FTIR experiments. Moreover, we shall see below that the thickness of the surface layer, although it is very small, exceeds that of the monolayer. Although crude, the estimate of a only few kelvins for the value of T_g is sufficient to explain that the $Fe^{3+}(S = {}^1/_2)$ ions remain paramagnetic when cooled to low temperatures. This small value of T_g also justifies the use of the simple Curie law to describe the spins of the surface layer for $T >$ 4 K, which amounts to neglect of correlations of the iron spins in the surface layer over the temperature range investigated in our experiments.

In some antiferromagnetic particles, the finite size may result in a different number of spins in each sublattice, producing a permanent magnetic moment or weak ferromagnetism.[21] Weak ferromagnetism was not evidenced in our materials, meaning that the opposite case, in which the particles consist of a core of spins with antiferromagnetic exchange interactions surrounded by a magnetically disordered shell, applied in our experiments. This is indeed the situation also met in Fe-based spinels, including $CoFe_2O_4$[22] and $NiFe_2O_4$.[23,24] In ferrite particles, however, the magnetization density m does not vanish in the core region, because of the different spin values on A and B sites of spinels. In that case, the spin disorder at the surface is evidenced as a layer with vanishing magnetization density, so that the "magnetic size" of the particles is usually smaller than the size of the particles as determined by electron microscopy or X-ray diffraction, giving independent, direct evidence of the surface spin-disorder effects.[25] In particular, this reduction in the magnetization density allowed for estimates of 7 and 12 Å for the thickness of the disordered layer in Ba-ferrite[26] and $CoFe_2O_4$,[22] respectively. However, in $LiFePO_4$ particles, where $m = 0$ even in the core region, the existence of a disordered layer at the surface should not necessarily lead to any decrease of the magnetic response. The presence of this property here thus has a different origin, namely, the fact that the spin disorder is associated with the change of the spin carried by the iron ions from high-spin $Fe^{2+}(S = 2)$ to low-spin $Fe^{3+}(S = {}^1/_2)$ in the surface layer. It is the smaller value of S in the disordered layer that is responsible for the smaller magnetic susceptibility.

As in the case of ferrites, it is possible to estimate the thickness of the disordered layer from the value $1 - y = 0.11$ we have determined. The volume of the unit cell of $LiFePO_4$ is 291 $Å^3$, and there are 4 formula units per unit cell. To simplify, we note that the density of iron atoms is the same as if the Fe atoms were distributed on a simple cubic lattice with lattice parameter a defined by the condition $a^3 = 291\ Å^3/4$, that is, $a = 4.17$ Å. A nanosphere of diameter $d = 30a$ composed of atoms forming a simple cubic lattice of parameter a has a surface-to-volume ratio of 0.16.[27] Since this ratio is approximately inversely proportional to d, a particle of diameter $d = 35$ nm $= 84a$, which is the typical size of the $LiFePO_4$ particles in the sample, then has a surface-to-volume ratio of 0.06. This is a factor of 2 smaller than the fraction $1 - y$ of iron ions in the $Fe^{3+}(S = {}^1/_2)$ state, i.e., in the surface layer, which means that the thickness of the disordered layer is typically only $2a \approx 8$ Å. A more quantitative estimate is beyond the present scope, since it would require taking into account the dispersion (i.e., the size distribution) of the particles as well as their shape, which is more complex than spherical. Nevertheless, this estimate is sufficient to confirm that the existence of the disordered spin layer and the related Fe^{3+} ions is indeed a surface effect, with a thickness of the disordered surface layer that is very similar to the situation met in ferrite nanoparticles.

In many cases it is difficult to demonstrate that the anomalous magnetic behavior of nanoparticles is localized at the surface rather than distributed throughout the bulk or associated with defects for very small particles on the order of 0.5–10 nm in size.[28] On the other hand, for particles with diameter $d > 10$ nm, it is usually believed that the smaller value of the magnetization is a result of the nature of the surface.[22] In the present study, the larger size of d ensures that this latter case applies. This is corroborated by the fact that both the XRD patterns and the FTIR spectra of the particles are the same as those for bulk $LiFePO_4$.

The evidence of Fe^{3+} at the surface of the $LiFePO_4$ nanoparticles conciliates the magnetic properties with prior Mössbauer experiments on this material that revealed the presence of a small percentage of iron in the Fe^{3+} state[29] that was not detected by XRD. In this earlier work, Andersson et al. suggested the possibility that an extremely thin noncrystalline phase boundary ran through the $LiFePO_4$ phase boundary, since the work was devoted to the study of partially delithiated samples rather than $LiFePO_4$ itself. They also invoked as an alternative explanation of their results the oxidation of iron from Fe^{2+} to Fe^{3+} without conversion to $FePO_4$. In refs 29 and 30, the relative concentration of Fe^{3+} was of the same order of magnitude but smaller than in the present sample, because the particles in the prior work were bigger.

Fe^{3+} is a natural ionization state of iron at many surfaces, which is actually very fortunate because it allows Fe^{3+} to serve as the active site for many catalytic reactions of

(21) Néel, L. In *Low Temperature Physics*; Dewitt, C., Dreyfus, B., De Gennes, P. G., Eds.; Gordon and Breach: New York, 1962.
(22) Lin, D.; Nunes, A. C.; Majkrzak, C. F.; Berkowitz, A. E. *J. Magn. Magn. Mater.* **1995**, *145*, 343.
(23) Morrish, A. H.; Haneda, K. J. *Appl. Phys.* **1981**, *52*, 2496.
(24) Komeda, R. H.; Berkowitz, A. E.; McNiff, E. J., Jr.; Foner, S. *Phys. Rev. Lett.* **1996**, *77*, 394.
(25) Rosensweig, R. E. *Ferrohydrodynamics*; Cambridge University Press: Cambridge, U.K., 1985; p 58.
(26) Rösler, M.; Görnert, P.; Sinn, E. *Z. Phys. D* **1991**, *19*, 279.
(27) Labaye, Y.; Crisan, O.; Berger, L.; Greneche, J. M.; Coey, J. M. *J. Appl. Phys.* **2002**, *91*, 8715.
(28) Nunes, A. C. *J. Appl. Crystallogr.* **1988**, *21*, 129.
(29) Andersson, A. S.; Kalska, B.; Häggström, L.; Thomas, J. O. *Solid State Ionics* **2000**, *130*, 41.
(30) Benoit, C. Ph.D. Dissertation, University Paris XIII-Orsay, July 2007.

importance in biological processes. This is the case, for instance, for proteins that contain heme Fe, such as the ferritin protein, where Fe^{3+} ions form crystallites together with phosphate and hydroxide ions, and the cytochrome P450 superfamily of enzymes, in which Fe^{3+} metabolizes many endogenous compounds, thus participating in the deactivation of many carcinogens as well as a number of xenobiotic compounds, including several drugs. This is indeed the reason why the cytochrome P450 superfamily has been extensively studied, and we have learned from these investigations that the heme Fe^{3+} is in the low-spin state when P450 is substrate-free[31] but in the high-spin state upon binding a substrate.[32] On the basis of this example among others, it is not surprising that the spin carried by Fe^{3+} at the $LiFePO_4$ surface depends on the coating of the particles. In the case investigated in the present work, the iron ions in the surface layer of the uncoated particles were in the low-spin state, as in substrate-free P450. But when the particles were carbon-coated, the material behaved like cytochrome P450, as the Fe^{3+} ions in the surface layer switched to the high-spin state. In the same spirit, magnetic and Mössbauer experiments have also determined that coating $NiFe_2O_4$ particles with an organic surfactant modifies the surface properties and the iron spin configuration in the surface layer.[33]

The absence of any Fe^{3+} compound in the XRD patterns and FTIR experiments on our sample corroborated the idea that the Fe^{3+} ions were embedded in an amorphous surface layer.[29] This is in the same spirit as the "X-ray invisible" amorphous Sn_2Fe component invoked to explain the larger amount of Sn_2Fe formed during the recharge of Li/Sn_2Fe cells measured by Mössbauer as opposed to X-ray analysis.[34,35] Models of spin-disordered surface layers in antiferromagnetic nanoparticles also consider a priori that the surface is amorphous.[20] However, the fact that XRD did not detect any Fe^{3+} compound cannot be considered as proof that the atoms at the surface were disordered because the thickness of the layer is so small that a geometric organization of Fe^{3+} would not be detected even if it existed. That is why FTIR experiments were important here, because FTIR spectroscopy is a probe of the order on a molecular-length scale and corroborated that the surface layer was indeed amorphous. This result, however, may depend also on the conditions under which the $LiFePO_4$ particles were prepared. At this stage, it is not possible to determine if the modification of the surface in the course of the carbon coating was due to the carbon deposit itself or to the sintering of the sample at 750 °C during this process. Investigation of calcination effects in the absence of any carbon additive is needed in order to distinguish between carbon-coating and sintering effects.

7. Conclusion

Uncoated $LiFePO_4$ nanoparticles have been prepared under conditions where the size of the particles is small enough that surface effects become important but large enough that their core region is not affected. The combination of XRD, FTIR, and magnetic measurements allowed us to demonstrate that the surface layer of the particles before carbon coating was amorphous and that the iron ions in this layer were in the Fe^{3+} low-spin configuration ($S = {}^1/_2$), forming a spin-disordered surface layer, while the $S = 2$ spins of the core region were coupled by antiferromagnetic interactions. These results suggest that at very low temperatures, the $LiFePO_4$ particles exhibit the properties of spin-glass surface disorder of antiferromagnetic particles that are of current interest in nanomagnetism. However, spin-glass freezing is expected to occur at a temperature $T_g \leq 4$ K in the present case, since the magnetic interactions were smaller than in the case of ferrites where such a behavior has been observed. In the temperature range 4−50 K explored in the present work, the $LiFePO_4$ particles had an antiferromagnetic core surrounded by a paramagnetic layer of Fe^{3+} spins. Some of the properties of the surface layer, including the low-spin versus high-spin state of Fe^{3+} in this layer, presumably are very dependent on the mode of preparation of the surface and on the carbon coating of the particles that is needed for use of the particles as a cathode element in lithium batteries. This dependence was already evidenced by the fact that Fe^{3+} switched from the low-spin to the high-spin state after carbon coating. However, comparison with the case of ferrites suggests that some basic properties, such as the thickness of the disordered layer (8 Å) and the trivalent configuration of iron at the surface, are robust. These results conciliate past Mössbauer spectroscopy measurements that detected a small percentage of Fe^{3+} ions, in apparent contradiction with other experiments. The present work suggests the need for further, more systematic investigations of the surface of these particles together with the impact of the surface on the electrochemical properties of these nanoparticles in relation to the mode of preparation.

CM7027993

(31) Kobayashi, K.; Amano, M.; Kanbara, Y.; Hayashi, K. *J. Biol. Chem.* **1987**, *262*, 5445.
(32) Schenkman, J. B.; Sligar, S. G.; Cinti, D. T. *Pharmacol. Ther.* **1981**, *12*, 43.
(33) Berkowitz, A. E.; Lahut, J. A.; Van Buren, C. E. *IEEE Trans. Magn.* **1980**, *16*, 184.
(34) Mao, O.; Dunlap, A.; Courtney, I. A.; Dahn, J. R. *J. Electrochem. Soc.* **1998**, *145*, 4195.
(35) Mao, O.; Dunlap, A.; Dahn, J. R. *Phys. Rev. B* **1999**, *59*, 3494.